



ISSN: 0067-2904

The Simulation of Old Human Remains Detecting Utilizing Ground Penetrating Radar Image Processing

Laith A. Jawad*, Alaa S. Mahdi, Faleh H. Mahmood

Remote Sensing Unit, College of Science, University of Baghdad, Baghdad, Iraq

Received: 19/1/2022

Accepted: 29/11/2022

Published: 30/9/2023

Abstract

Many Iraqi provinces had collective cemeteries, especially in the middle and southern regions of Iraq, but many of those cemetery locations are undefined yet. Ground penetration radar has two features that make it optimal from a geophysical perspective for shallowly detecting sensitive materials near the surface. First, the instantaneous image is formed upon scanning, called a radargram. Second, the non-destructive inference of the scanned materials. For these two reasons, this technique was chosen to conduct a simulation process to reveal the old human remains in Iraq's central and southern areas using another model with the same physical feature (old burial) at the AL-Khamisiya site, Thi-Qar province.

The demanded stages for completing the simulation process can be divided into two parts. The first part is that before the model's burial, a field survey was conducted to identify the site subsurface features and test the penetration extent of the selected antennas, in addition, to accurately calculating the speed of radar phase waves to obtain a calibrated measurement of the target's depth of burial. After the model's burying (the remains of old Iraqi humans), the second part included individual scanning and grouping at a depth of two m and four m.

This simulation proved that the variation value in the dielectric constant between the burial medium (host medium) and the buried body (target) is the most critical determinant of detecting the remains' success or failure. Also, the work proved that low frequencies between (100-250) MHz are optimal for detecting human remains in a saline environment.

Keywords: old remains, simulation process, dielectric constant

محاكاة للكشف عن الرفات البشرية القديمة باستخدام معالجة صور الرادار المخترقة للأرض

ليث عزيز جواد*، علاء سعود مهدي، فالح حسن محمود

وحدة الاستشعار عن بعد، كلية العلوم، جامعة بغداد، بغداد، العراق

الخلاصة

تحتوي العديد من المحافظات العراقية على مقابر جماعية خاصة في المناطق الوسطى والجنوبية من العراق ، لكن الكثير من هذه المقابر لم يتم تحديدها بعد. يحتوي رادار اختراق الأرض على ميزتين تجعله مثاليًا من منظور جيوفيزيائي للكشف الضحل عن المواد شديدة الحساسية بالقرب من السطح ؛ الأول هو الصورة اللحظية التي تتكون عند المسح ، والتي تسمى Radargram ، والثانية هي الاستدلال غير الأتلافي للمواد الممسوحة رادارياً. لهذا السبب ، تم اختيار هذه التقنية لإجراء عملية المحاكاة في الكشف عن رفات البشر القدامى في

*Email: laith1910saadi@gmail.com

المناطق الوسطى والجنوبية من العراق باستخدام نموذج آخر بنفس السمة المادية (الدفن القديم) في موقع الخميسية من محافظة ذي قار .
 يمكن تقسيم المراحل المطلوبة لإكمال عملية المحاكاة إلى جزأين ، الجزء الأول قبل دفن النموذج ويتضمن مسحًا ميدانيًا لتحديد السمات ما تحت السطحية للموقع ومدى اختراق كل من ترددي الهوائيات المختارة من أجل المشروع، بالإضافة إلى حساب سرعة طورالموجة الرادارية بدقة في هذا الموقع للحصول على قياس معايير لعمق دفن الأهداف. اما الجزء الثاني بعد دفن النماذج (رفات عراقيين قديمة) فقد اشتمل على مسح للرفات بشكل فردي وتجميعي على عمق مترين ثم على عمق اربعة امتار .
 أثبتت هذه المحاكاة أن قيمة التباين في ثابت العزل الكهربائي بين وسط الدفن (الوسط المضيف) والجسم المدفون (الهدف) هو المحدد الأهم لنجاح أو فشل عملية الكشف عن البقايا بهذه التقنية ، وكذلك العمل أثبت أن الترددات المنخفضة بين (100-250) MHz هي الأمثل للكشف عن الرفات البشرية في بيئة.

1. Introduction

Subsurface Interface Radar (SIR), Ground Impulse Radar (GIR)[1], Ground Probing Radar (GPR) [2], or Ground Penetration Radar (GPR) are named for the similar technique that forms radargram profile (shallow image of subsurface features) utilizing microwave EM pulses [3]. The (UHF or VHF) Freq.s of microwave band is used scheme to achieve a remotely sensed Non-Destructive Technique (NDT) subsurface scan [4] so that it is optimum for highly sensitive media surveying (i.e., special features protecting or risky features' avoiding). The valid frequencies of GPR fall between ten to thousand MHz [5].

A sequence pulse is emitted to the ground surface from the GPR transmitter when it encounters a target and two layers interface (the layers varying by magnetic permeability, electric permittivity, or electric conductivity) [6]. The pulse scattered, refracted, and reflected. This technique was first used by adopting micro radar pulses to find burials, Hülsenbeeck in 1926 [7].

The existence of voids (soil is not compressed), medium conductivity (because of water or salinity), and user experience lack are influencing the efficiency of GPR detection [8].

The GPR receiver captures the reflected signals from shallow targets, then the control unit records and manages it in a longitudinal sample of radar data called a trace stands for amplitude versus signal in the device displaying unit. Stacked series of traces, commonly called radargram profiles, are generated with the device moving in the field [9].

GPR Data's general Processing steps are:

- Direct and airwave minimization from the signal.
- Amplitude adjusting.
- Gain modifying.
- Signal distance Normalizing.
- Horizontal scale adjusting.
- Filtration of any vertical frequencies.
- Phase velocity calibrating.
- Migrating process achievement.

The radargram image is more interpretable when noisy signals are removed, enhancing the exciting features' brightness [10].

2. Materials and Methods

Electromagnetic waves from the device transmitter propagate under the earth's surface in a conical shape with little energy at a rate inversely proportional to the square of the distance from the transmitter [11]. The reasons for the low energy of the radar pulse are the magnetic permeability (μ), the angular frequency (ω), the electrical conductivity (σ), as well as the electrical permittivity (ϵ), which is the most critical factor in reducing the energy of the electromagnetic waves of the GPR, those reasons gathered in one equation [12]:

$$\alpha = \omega[\mu_a \epsilon_a \{(1 + \sigma^2/\omega^2 \epsilon_a^2) - 1\}/2]^{1/2} \dots (1)$$

Where: (α) is the attenuation factor.

Table 1: Notable features with their radar parameters and physical aspects [13].

Material	ϵ	σ m S/M	V M/ n S	α dB/M
Air	1	0	0.3	0
Ice	3-4	0.01	0.16	0.01
Fresh water	80	0.05	0.033	0.1
Salt water	80	3000	0.01	1000
Dry sand	3-5	0.01	0.15	0.01
Wet sand	20-30	0.01-1	0.06	0.03-0.3
Shales and clay	5-20	1-1000	0.08	1-100
Silt	5-30	1-100	0.07	1-100
limestone	4-8	0.5-2	0.12	0.4-1
Granit	4-6	0.01-1	0.13	0.01-1
(Dry) salt	5-6	0.01-1	0.13	0.01-1

The study area is in Hawr Al-Khamisiya of Thi Qar province, called the Al-Khamisiya site. As shown in Figure (1), a Topcon Hyper-II DGPS was used to determine the area's boundaries, which eyewitnesses designated; it extends between the northern latitudes 30° 44'12.509" and 30°45'47.082". The eastern longitude is 46°26'13.25" and 46°28'42.604", with an area of 5.3 km². The Third River (the broad estuary) passes near it, which is the main reason for the area's salinity due to the saline drainage water collection from farms in the central and southern parts of Iraq.

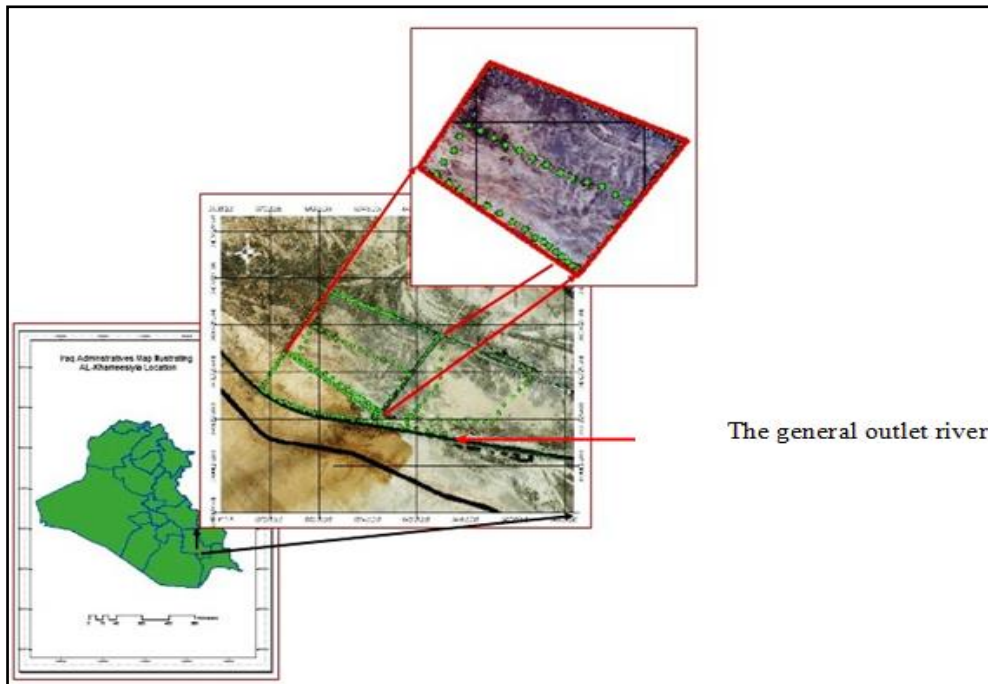


Figure1: Map showing the location of the study area using the actual “Quick Bird” composite band imagery with area borders delineated by green points.

The work aims to detect old human remains in a salinity environment using Ground Penetrating Radar (GPR). Old Iraqi martyr remains saved from 1986 were used as samples. The reflected radar data was simulated in Iraq's central and southern parts. Human remains subjected to sufficient time for dissolution were buried at shallow depths individually or collectively for extended periods. The antennas used had frequencies of (250 and 500) MHz, and the burial depths were two and four meters, respectively. The remains of individual and grouped Iraqi martyrs were placed in each pit during every survey process, as seen in Figure (2).



Figure2: The burying process of Iraqi martyrs remains at four meters depth.

In this simulation, the start point was the pre-drill test of underground media to state if there were any interlayer anomalies in the area of interest and measure the penetration depth of each antenna, as seen in Figures (3) and (4).

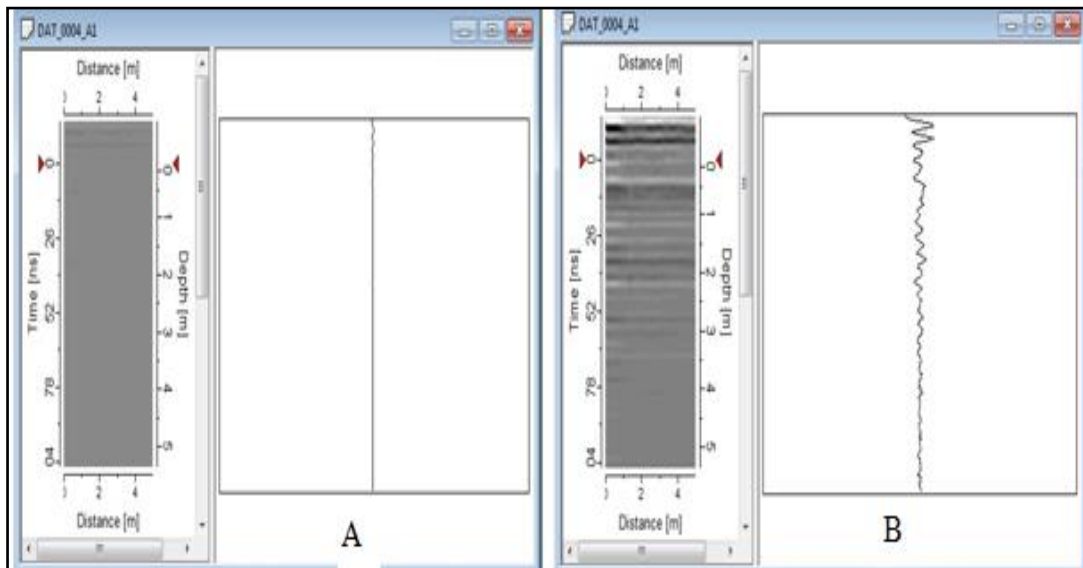


Figure 3: A-The preprocessed radar profile image of the Al-Khamisiya site using a 250 MHz antenna

B- The processed radar profile image of the Al-Khamisiya site using a 250 MHz antenna

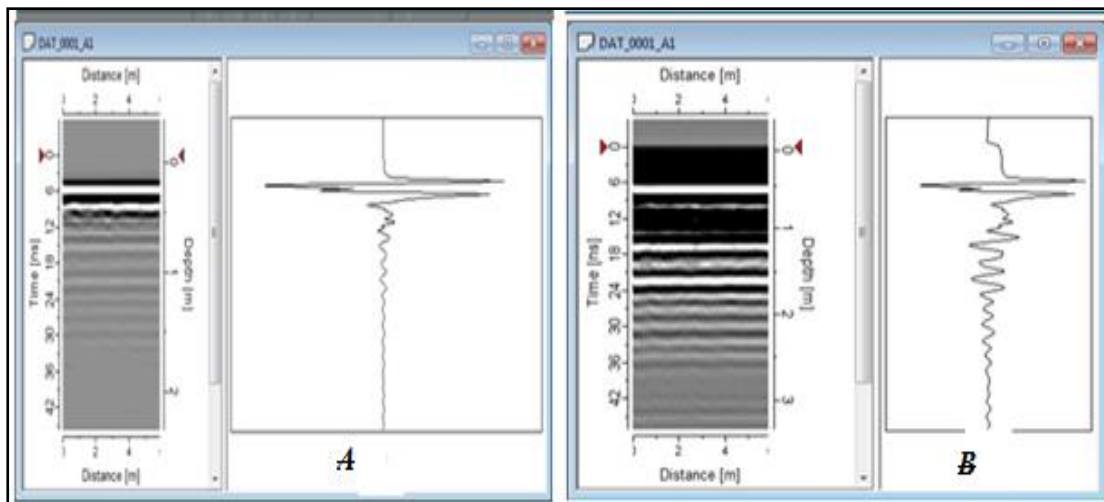


Figure 4: A-The preprocessed radar profile image of the Al-Khamisiya site using a 500 MHz antenna

B- The processed radar profile image of the Al-Khamisiya site using a 500 MHz antenna

The pre-drilling test showed the absence of voids or solid targets in the soil subsurface, which does not lead to anomalies in the radar images of the site under study. This test also showed that the approximate penetration depth of the radar wave is 4.5 m for a frequency of 250 MHz and less than approximately 3 m using a 500 MHz antenna.

After that, the electromagnetic wave phase velocity value was extracted for the relevant site (the process is critical to calibrate the depth of the field-scanned targets). The appropriate program to extract the velocity was not available when conducting the simulation, so it was

replaced by placing a piece of highly conductive material at a depth of two meters (a known depth) to determine the speed of the radar wave near the surface, Figures (5) and (6).

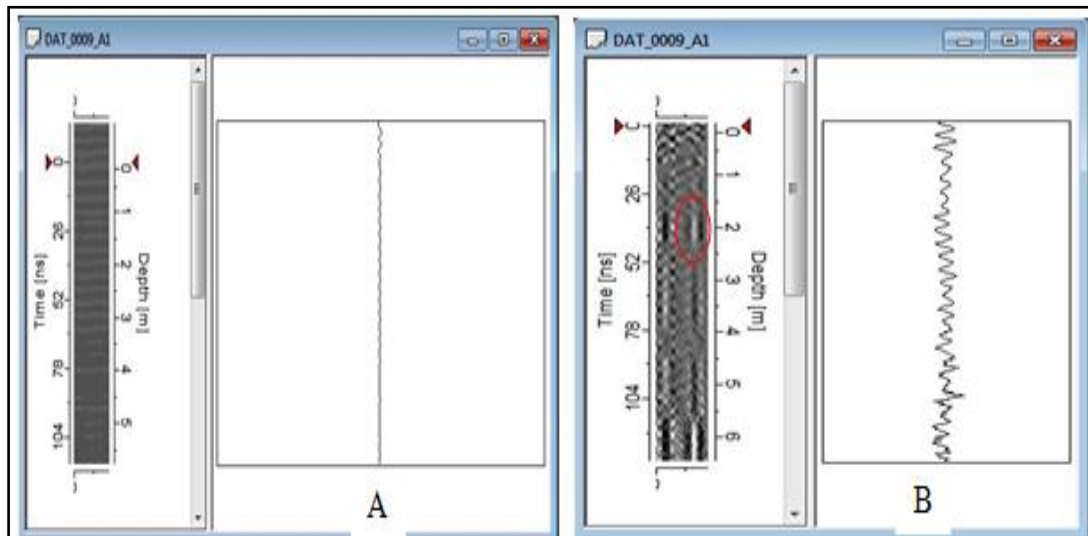


Figure 5: (A) The pre-processed soil with iron piece radargram using 250 MHz; (B) The processed soil with iron piece radargram using 250 MHz

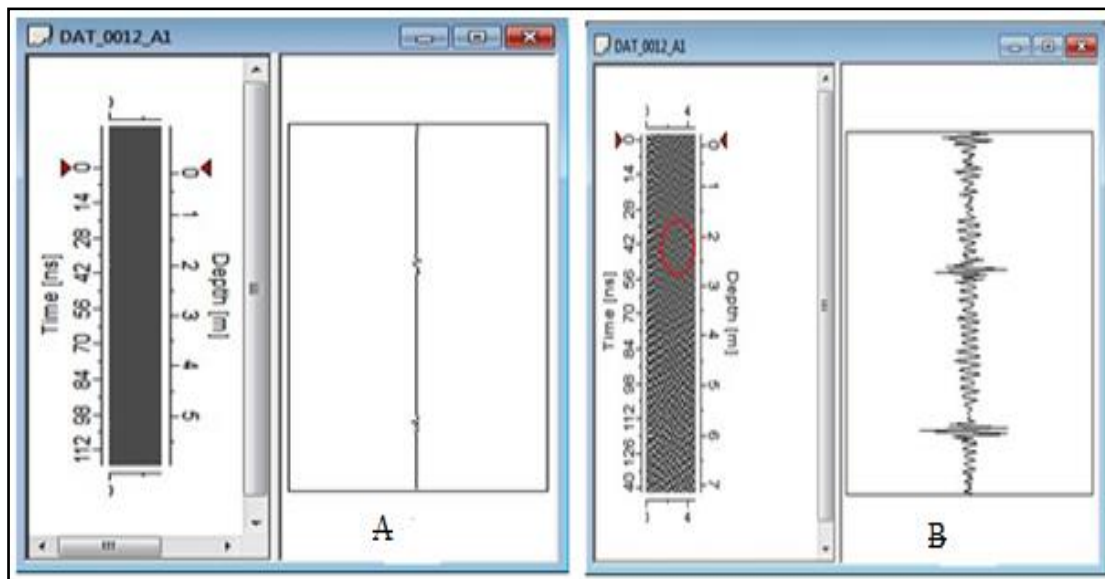


Figure 6. (A) The pre-processed soil with iron piece radargram using 500 MHz; (B) The processed soil with iron piece radargram using 500 MHz

At the simulation site, it was found that the velocity of the penetrating wave was 140 nm/sec. Then a crevice was dug in the ground, a meter wide and two meters deep, and the burial process was carried out for the remains of the Iraqi martyrs once individually and collectively. For each burial, the scanning process was conducted with a GPR device at 250 MHz and 500 MHz, respectively, as shown in Figures (7) and (8):

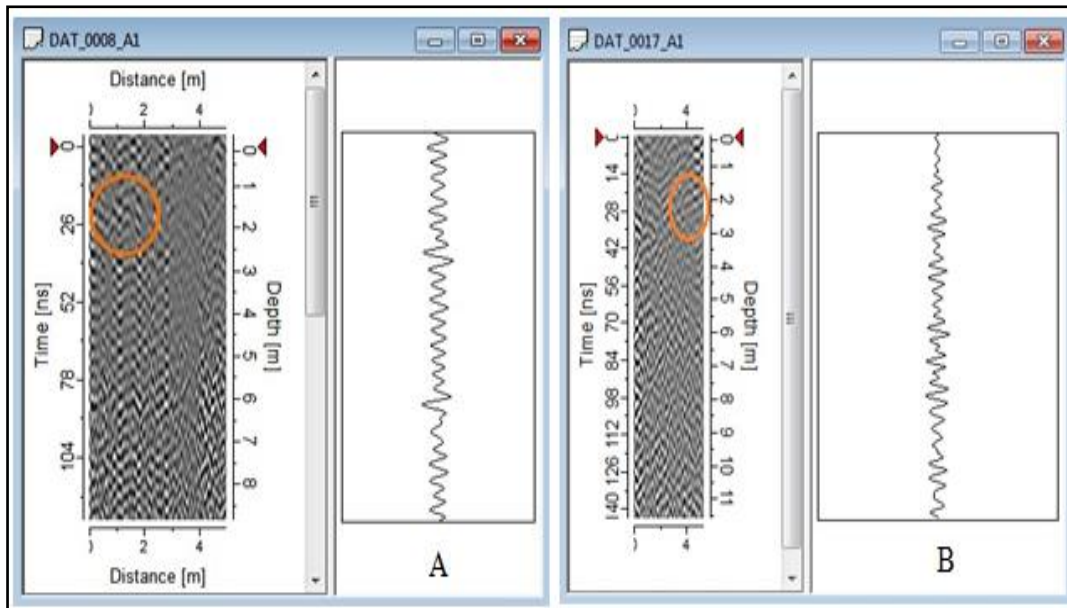


Figure 7: (A) The processed profile image for one mortal utilizing 250 MHz;
 (B) The processed profile image for one mortal utilizing 500 MHz

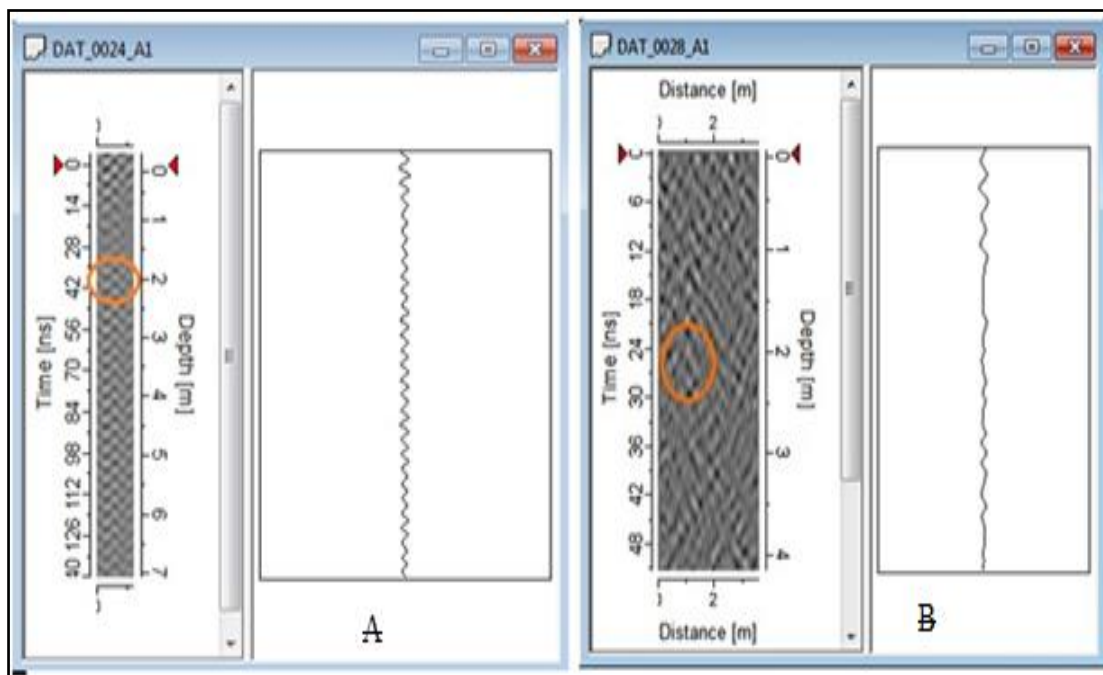


Figure 8: (A) The processed profile image for grouped mortal utilizing 250 MHz;
 (B) The processed profile image for grouped mortal utilizing 500 MHz

The last step in the simulation process was a crevice dug in the ground a meter wide and four meters deep. Figures (9) and (10) were the same procedures.

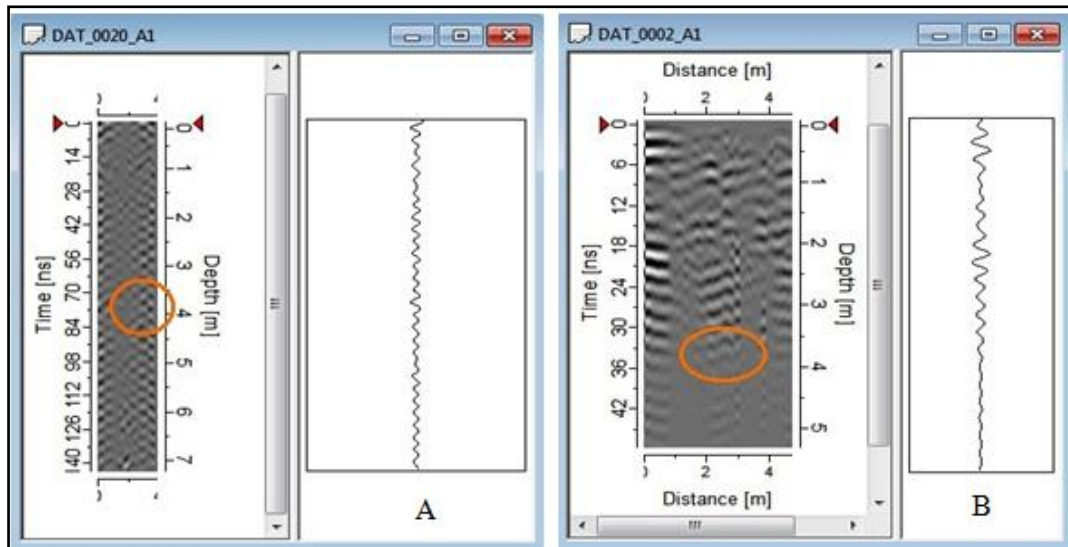


Figure 9: (A) The processed image for one body utilizing 250 MHz
 (B) The processed image for one body utilizing using 500 MHz

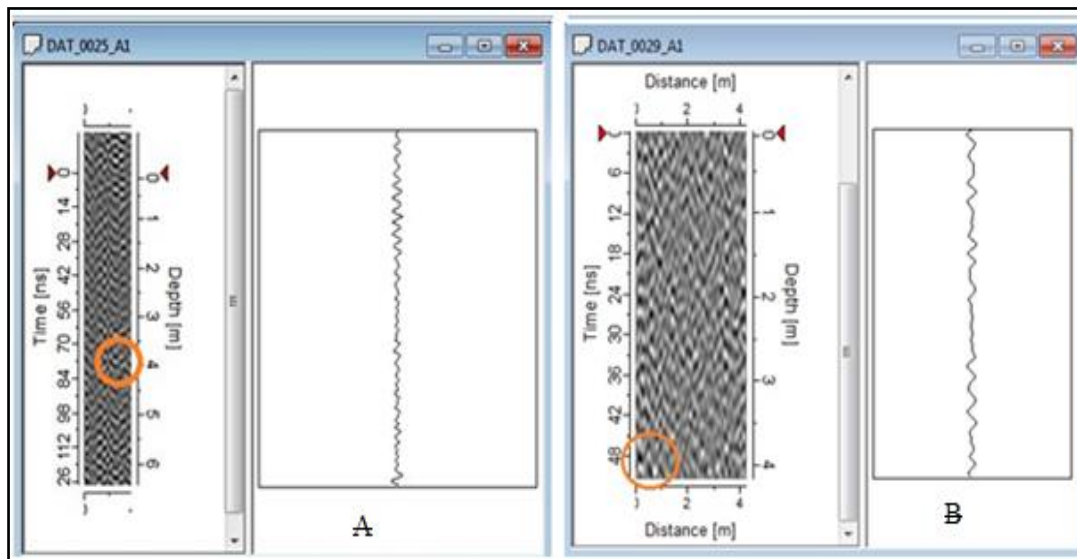


Figure 10: (A) The processed image for grouped bodies utilizing 250 MHz
 (B) The processed image for grouped bodies utilizing 500 MHz

For the Al- Khamisiya site, the radar profile processing starts with a clearance of air distance that separates the antenna from the surface, then calibrating the depth gauge using the calculated mean phase velocity of the host. The following filters (DC signal remove, background remove, auto-gain, band-pass, and run-average) were utilized, respectively. Filters were implemented to overcome environmental conditions that reduce radar pulse signal, such as high soil conductivity due to shallow groundwater movement up to the surface and the leakage of saline irrigation water from the “third river” district and voids increment as a result of stirring.

3. Results and Discussion

This part of the research shows the results obtained from the analysis process as follows:

a. Interest region penetration depth:

The depth of pulse penetration of the GPR decreased from approximately 4.5 m using a 250 MHz antenna to about 3 m using a 500 MHz antenna. It is due to the doubling of attenuation value (α) of the radar signal, equation (1), which has been proved in the pre-drill test of the underground media and illustrated in Figures (3) and (4).

b. The first burial depth testing:

Images obtained at a depth of two meters from antennas appeared similarly, with the presence of hyperbolas that were not precisely clear during the burying of the individual and grouping samples. That was due to the lack of variation in soil dielectric constant values from remains attributing to the length of the burial period that led to dissolution; it was the reason for the small amplitude of the reflected pulse, see Figures (7) and (8).

c. The second burial depth testing:

Burying at a depth of 4 m, the radar image of the GPR and for the two models (individual or group burial) contained inaccurate cuts with an echo in the image when using a frequency of 250, but in the case of 500, the resulting image is distorted, due to the significant attenuation factors as shown by equation (2).

4. Conclusions

The research showed that the amplitude value of reflected GPR pulse is mainly determined by the value of discrepancy between the isolation constant of the host medium and the target in which it is buried, confirming the increase in the chances of detecting the remains as the time interval between burial and detection decreases. Moreover, it was proved through the simulation process that the saline environment of the Al-Khamisiya site (which is slightly more saline than the usual environment for the central and southern regions of Iraq because of the interest region neighboring the highly saline Third River) effectively affects the penetration depth of the electromagnetic pulse of the GPR device. The penetration depth was 4.5 m at a frequency of 250 and decreased to about 3 m using a frequency of 500 MHz. Therefore, this technique is efficient and can determine the presence of human remains in a harsh environment, especially by reducing the frequency. For example, using an antenna with a frequency of 100, it is unreasonable to establish individual or collective graves with a depth of more than 4.5 m.

References

- [1] Sun J., Young R.A., "Recognizing surface scattering in ground-penetrating radar data.", *Journal of Geophysics*, vol. 2, no.60, pp. 1378–1385, 1995
- [2] Perez V., Caselles O., Salinas V., Pujades L.G., Clapé s J., "GPR applications in dense cities: Detection of paleochannels and infilled torrents in Barcelona GPR applications in dense cities," *Proceedings of the IEEE 13th Int. Conf. on Ground Penetrating Radar (GPR)*, Lecce, Italy, pp. 1–5. 21–25 June, 2010
- [3] Harbi H., McMechan G.A., "Conductivity and scattering Q in GPR data: Example from the Ellenburger dolomite, central Texas", *Journal of Geophysics*, vol.3, no.77, pp. 63–78, 2012
- [4] Santos S., Perez V., Gonzalez R., "GPR backscattering applied to urban shallow geology: GPR application in seismic microzonation", *Proceedings of the IEEE 8th International Workshop on Advanced Ground Penetrating Radar (IWAGPR)*, Florence, Italy, pp. 1–4, 7–10 July, 2015
- [5] Chandler V.W., Lively R.S., "Utility of the horizontal-to-vertical spectral ratio passive seismic method for estimating thickness of Quaternary sediments in Minnesota and adjacent parts of Wisconsin" *Interpretation*, vol.4, no. 3, pp. 71–90, 2016
- [6] Takahashi K., Igel J., Preetz H., Sato M., "Sensitivity analysis of soil heterogeneity for ground—penetrating radar measurements by means of a simple modeling", *Journal of Radio Science*, vol. 50, no.2, pp. 79–86, 2015

- [7] Panzera F., D'Amico S., Lombardo G., Longo E., "Evaluation of building fundamental periods and effects of local geology on ground motion parameters in the Siracusa area, Italy", *Journal of Seismology*, vol. 2, no. 20, pp. 1001–1019, 2019
- [8] Jawad L.A., Huda W. A., "The Al-Abiadh Valley Drainage Basin Environmental Aspects Extraction Using Quantitatively Morphometric Analyses of Shuttle Radar Topographic Mission Data," *Baghdad Science Journal*, vol.16, no., pp.197-103, 2019
- [9] Anas A. M., Jawad L.A., Faleh H. M., "The Use of Ground Penetrating Radar to Assess the Concrete", *Iraqi Journal Science*. Vol. 60, no.9, pp. 2095-2101, 2019
- [10] Cornick M., Koechling J., Stanley B., Zhang B., "Localizing ground penetrating RADAR: A step toward robust autonomous ground vehicle localization", *Journal of Field Robotics*, vol. 33, no. 1, pp. 82–102, 2016
- [11] Leuschen C.J., Plumb R.G., "Matched-Filter-Based Reverse-Time Migration Algorithm for Ground-Penetrating Radar Data", *IEEE Journal of Trans. Geosciences Remote Sensing*, vol. 39, no. 5, pp. 929 – 936, 2001
- [12] Jawad L.A., "Demonstration of Net Solar Radiation Geographical Behavior Revers Correlation with Relative Humidity in Iraq", *Iraqi Journal Science*. vol. 63, no.6, pp. 2741-2754, 2022
- [13] Grasmueck M., Weger R., Horstmeyer H., "Three-dimensional ground-penetrating radar imaging of sedimentary structures, fractures, and archaeological features at submeter resolution", *Journal of Geology*, vol. 32, no.6, pp. 933–936, 2004